NRC Research Press

ARTICLE

The reaction mechanism of chiral hydroxylation of *p*-OH and *p*-NH_2 substituted compounds by ethylbenzene dehydrogenase

Agnieszka Dudzik, Bartłomiej Kozik, Mateusz Tataruch, Anna Wójcik, Daniel Knack, Tomasz Borowski, Johann Heider, Małgorzata Witko, and Maciej Szaleniec

Abstract: Ethylbenzene dehydrogenase (EbDH; enzyme commission (EC) number: 1.17.99.2) is a unique biocatalyst that hydroxylates alkylaromatic and alkylheterocyclic compounds to (*S*)-secondary alcohols under anaerobic conditions. The enzyme exhibits a high promiscuity catalyzing oxidation of over 30 substrates, inter alia, para-substituted alkylphenols and alkylanilines. Secondary alcohols with OH and NH_2 substituents in the aromatic ring are highly valuable synthons for many biologically active compounds in the fine chemical industry. EbDH hydroxylates most of the studied compounds highly enantioselectively, except for five substrates that harbour OH and NH_2 groups in the para position, which exhibit a significant decrease in the percent enantiomeric excess (% ee). This phenomenon is inconsistent with the previously suggested enzyme mechanism, but it may be linked to a stabilization of the carbocation intermediate by deprotonation of the OH or NH_2 substituent in the active site that yields a transient quinone (imine) ethide species. This would initiate an alternative reaction pathway involving the addition of a water molecule to a C=C double bond. This hypothesis was cross-validated by density functional theory (DFT) cluster modelling of the alternative reaction pathway with 4-ethylphenol, as well as by experimental assessment of the pH dependency of enantiomeric excesses. The results reported herein suggest that the alternative reaction pathway may significantly contribute to the overall reaction if the carbocation intermediates are stabilized by deprotonation.

Key words: ethylbenzene dehydrogenase, molybdenum enzyme, chiral alcohols, DFT.

Résumé : L'éthylbenzène dehydrogenase (EC 1.17.99.2) est un biocatalyseur unique qui hydroxyle les composés alkylaromatiques et alkyl hétérocycliques pour donner des énantiomères *S* d'alcools secondaires dans des conditions anaérobies. L'enzyme manifeste une importante promiscuité, catalysant l'oxydation de plus de 30 substrats, entre autres des alkylphénols et des alkylanilines substitués en *para*. Les alcools secondaires possédant des substituants OH et NH2 sur le noyau aromatique sont des synthons très utiles pour de nombreux composés biologiquement actifs dans l'industrie des produits de chimie fine. L'éthylbenzène hydroxylase hydroxyle de manière très énantiosélective la plupart des composés étudiés, excepté cinq substrats porteurs de groupements OH et NH_2 en position *para*, pour lesquels on observe une diminution significative de l'excès énantiomérique (ee %). Ce phénomène ne concorde pas avec le mécanisme enzymatique proposé antérieurement, mais il pourrait être lié à une stabilisation des carbocations intermédiaires par déprotonation du substituant OH ou NH_2 au site actif donnant une espèce éthide de quinone (imine) transitoire. Cela ouvrirait un autre chemin de réaction comprenant l'ajout d'une molécule d'eau sur une double liaison C=C. On a procédé à une validation croisée de cette hypothèse par modélisation, fondée sur la théorie de la fonctionnelle de la densité (DFT) et un modèle d'agrégat, du chemin de réaction de rechange avec le 4-éthylphénol, ainsi que par évaluation expérimentale de la dépendance des excès énantiométriques au pH. Les résultats présentés donnent à penser que le chemin de réaction de rechange pourrait contribuer considérablement à la réaction globale si les carbocations intermédiaires sont stabilisés par déprotonation. [Traduit par la Rédaction]

Mots-clés : éthylbenzène hydrolase, enzyme à molybdène, alcools chiraux, DFT.

Introduction

Ethylbenzene dehydrogenase (EbDH) is a molybdoenzyme belonging to the dimethyl sulfoxide (DMSO) reductase family,[1,2] and catalyzes the oxygen-independent, stereoselective hydroxylation of ethylbenzene to (*S*)-1-phenylethanol. It is the first known enzyme capable of direct anaerobic hydroxylation of a nonactivated hydrocarbon,[1,3,4] and is involved in the mineralization of ethylbenzene by *Aromatoleum aromaticum*, a denitrifying betaproteobacterium.[5] EbDH is a $\alpha\beta\gamma$ heterotrimer with subunits of 96, 43, and 23 kDa and contains a molybdenum cofactor and a heme b_{559} cofactor linked by a linear row of five iron–sulfur clusters.[6] The enzyme active site is deeply buried in the α subunit and is comprised of the molybdenum cofactor (MGD) and the side chains of aspartic acid 223 (Asp^{223}) and histidine 192 (His^{192}), which were proposed to be involved in the catalytic process.[6,7]

Our previous investigations have shown that EbDH hydroxylates aliphatic methylene groups adjacent to aromatic or heterocyclic rings in many different substrates, forming the respective secondary alcohols.[8–12] The implementation of chiral chromatography revealed that EbDH exhibits 100% reaction enan-

Received 13 December 2012. Accepted 18 March 2013.

A. Dudzik, M. Tataruch, A. Wójcik, T. Borowski, M. Witko, and M. Szaleniec. Jerzy Haber Institute of Catalysis and Surface Chemistry Polish Academy of Sciences Niezapominajek 8, 30-239 Kraków, Poland.
B. Kozik. Department of Organic Chemistry, Jagiellonian University, Ingardena 3, 30-060 Kraków, Poland.
D. Knack. Jerzy Haber Institute of Catalysis and Surface Chemistry Polish Academy of Sciences Niezapominajek 8, 30-239 Kraków, Poland; Laboratory for Microbial Biochemistry, Philipps University of Marburg, Karl-von-Frisch Strasse 8, D-35043 Marburg, Germany.
J. Heider. Laboratory for Microbial Biochemistry, Philipps University of Marburg, Karl-von-Frisch Strasse 8, D-35043 Marburg, Germany.
Corresponding author: Maciej Szaleniec (e-mail: ncszalen@cyfronet.pl).

This article is part of a Special Issue dedicated to Professor Dennis Salahub in recognition of his contributions to theoretical and computational chemistry.

"Friendship is the golden ribbon that ties the world together." Dennis, you are that ribbon.

Fig. 1. Proposed catalytic mechanism of ethylbenzene hydroxylation by EbDH. The molybdenum cofactor of EbDH is represented only by the Mo atom with its oxo or hydroxyl ligands. The respective molybdenum cofactor (MoCo) oxidation states are indicated. **S**, substrate state; **TS1**, transition state 1; **I**, intermediate state with bound radical; **I•**, alternative intermediate state with bound carbocation; **TS2**, transition state 2; **P**, product state.[7]

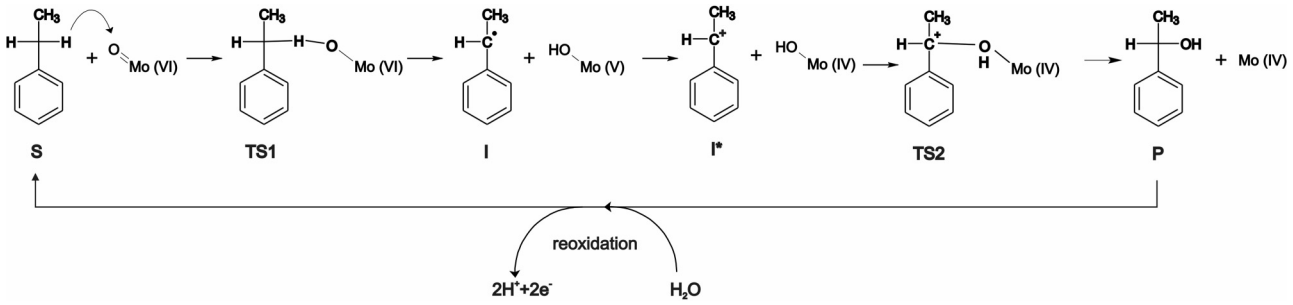

tioselectivity (within detection limits) for most compounds, yielding exclusively (*S*)-alcoholic products. For some substrates, however, substantial amounts of (*R*)-alcohols were also detected, although always as a minor fraction.[10] The theoretical studies of EbDH led to the formulation of a reaction mechanism, which appears to be valid for a majority of substrates. In short, the two-electron oxidation proceeds in two steps: (*i*) a radical type activation of the pro(*S*) C–H bond at C1 (**TS1**) leading to the formation of a radical intermediate (**I**) and reduction of Mo(VI) to Mo(V), and (*ii*) a second electron transfer coupled with subsequent OH rebound (**TS2**) leading to the formation of the alcohol product and reduction of Mo(V) to Mo(IV) (see Fig. 1). The extent of the radical or carbonation nature of the intermediate seems to depend on the substrate electronic characteristic,[13] as recent investigation of the reaction mechanism with the quantum mechanics/molecular mechanics (QM/MM) technique suggests a strong stabilization of the carbocation form of **I** introduced by the protein part of the enzyme.[14]

Pure chiral alcohols are universal synthons for the industrial production of fine chemicals and can be used as starting material for the development of new drugs, odorants, food additives, or even chiral nematic liquid crystals.[15–19] Therefore, EbDH has great potential for biotechnological applications and elucidation of its enantioselectivity with different substrates is of interest. The production of chiral alcohols by irreversible hydroxylation of hydrocarbons by EbDH is novel and complementary to the established process using alcohol dehydrogenases, which catalyze the reduction of ketones in a reversible manner. As a result, compounds with substituents promoting oxidation (i.e., electron donating groups) are enhancing the reaction rate of EbDH, precisely opposite to their influence on ketone reduction.[20,21] The *p*-OH and *p*-NH_2 electron donating effects enhancing reaction rates of EbDH are especially noteworthy for the synthesis of potential adrenaline analogues. However, the enhanced hydroxylation rate by EbDH observed for 4-ethylphenol (**4**) and 4-ethylaniline (**9**) was associated with a marked decrease of the reaction enantioselectivity.

Therefore, we have investigated, with experimental and theoretical techniques, the influence of the position of OH and NH_2 in the aromatic system on reaction enantioselectivity. The stereochemistry of the products was determined with chiral liquid chromatography (LC–mass spectrometry (MS)), while quantum chemical modelling was used to understand the experimentally observed phenomena. Alternative pathways were considered that are analogous to the one proposed for 4-ethylphenol methylenehydroxylase (4EPMH) from *Pseudomonas putida*.[22] 4EPMH hydroxylates 4-ethylphenol in two steps: (*i*) two electron oxidation with proton subtraction yields quinone ethide and (*ii*) water addition to the double bond takes place with concomitant protonation of the phenolic group. Re-evaluation of the structure of the active site of EbDH revealed a conveniently positioned residue, i.e., Asp^{485}, which would be available to form a hydrogen bond with the *p*-OH or -NH_2 substituents of the substrate analogues. Rotation of the side chain of this Asp would allow the carboxylic group to form hydrogen bonds with the substrate and the bound intermediates (Fig. 2).

The plausibility of the standard and the alternative reaction pathways leading to both (*R*)- and (*S*)-alcohols from 4-ethylphenol was assessed on the basis of density functional theory (DFT) modelling using small active site cluster models.

Experimental section

Sample preparation

Ethylbenzene dehydrogenase was purified from ethylbenzene-grown cells of *A. aromaticum* as described previously.[9,24] The enzyme assays were routinely conducted at an optimum pH of 7.5 at 30 °C in 20 mL of 100 mmol/L Tris/HCl containing 200 μmol/L ferricenium(III) tetrafluoroborate, and ethylbenzene dehydrogenase (100–300 μL of ~1 mg/mL protein solution). The reactions were initiated by adding 100 μL of a stock solution of the respective substrate in *tert*-butanol (a list of substrates, their purities and producers is available in the Supplementary data). After overnight incubation, the reaction mixtures where extracted from the water phase by solid phase extraction using either C18 Polar Plus (Baker) or polystyrene/divinylbenzene (PS/DVB) copolymer solid-phase extraction (SPE) columns (Strata-X from Phenomenex or the equivalent Chromabond HR-X from Macherey-Nagel), which were eluted with 0.5 mL of isopropanol.

Organic synthesis of standards

Syntheses of chiral standards and their racemic mixtures of 2-(1-hydroxyethyl)phenol (**II**), 3-(1-hydroxyethyl)phenol (**III**), 4-(1-hydroxyethyl)phenol (**IV**), and 4-(1-hydroxyprop-1-yl)phenol (**VI**) were previously described.[10] The (*S*)-2,3-dihydro-1*H*-indene-1,6-diol (**XIb**) was obtained by enzymatic reduction of 6-hydroxy-2,3-dihydro-1*H*-inden-1-one using recombinant (*S*)-specific phenylethanol dehydrogenase from *A. aromaticum*.[25,26]

Tests for pH dependency

The influence of the pH on the enantioselectivity of the reaction was investigated for 4-ethylphenol (**4**), 4-ethylaniline (**9**), and 2,3-dihydro-1*H*-inden-5-amine (**12**) to validate the proposed hypothesis involving a modified mechanism. Reactions were performed in 100 mmol/L Tris/HCl at pH values of 7.0, 7.5, or 8.0. The reaction products were separated and quantified by chiral chromatography using a normal-phase (NP) column with an atmosphere-pressure chemical ionization (APCI)-LC–MS instrument using both a diode-array detector (DAD) and selected-ion monitoring (SIM).

LC/LC–MS

The chiral high-performance liquid chromatography (HPLC) separations were performed on an Agilent 1100 system in a normal-phase system on a cellulose tribenzoate polysaccharide chiral stationary phase (Daicel CHIRALCEL OB-H column, 250 mm ×

Fig. 2. Model of the structure of the active site of EbDH during C–H activation of 4-ethylphenol (**4**). The position of the Asp^{485} side chain was manually modified by rotation of the Cα and Cβ dihedral angle by +190°, and the position of the substrate was derived from that of ethylbenzene in **TS1** from the QM/MM calculations.[23]

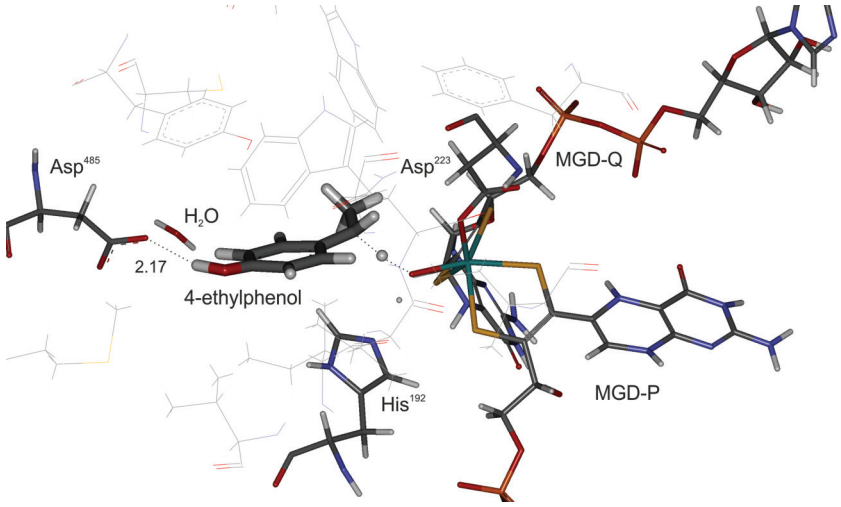

4.6 mm, 5 μm). To avoid changes in sample concentrations during the analysis, the autosampler was thermostated to 8 °C. Depending on the polarity of analytes, different types of uniform isocratic programs were used with mobile phases comprised of mixtures of *n*-hexane/isopropanol in ratios ranging from 90:10 up to 65:35 (*v*/*v*) (see Table 1) at 25 °C and at a flow rate of 0.5 mL/min. Products were detected by a DAD (Agilent 1100 DAD) with or without coupling to an MS detector (VL MS spectrometer) using an APCI ion source in positive or negative ion mode (Table S1 in the Supplementary data). The mobile phase used in the normal-phase chromatography (i.e., with a high *n*-hexane concentration) is widely regarded as incompatible with the APCI due to the high hazard of *n*-hexane explosion upon contact with heated nebulizer and high voltage corona discharge.[27] Moreover, a high content of *n*-hexane and lack of ions in the mobile phase decreases the chance of sample ionization with APCI and destabilizes the mass spectrometer (system instability and over polarization due to the uncontrolled electric discharges were observed). Therefore, we used a modified method of Zavitsanos and co-workers[27,28] to couple a normal mobile phase with APCI-MS by 1:1 post column addition (i.e., 0.5 mL/min) of 25 mmol/L $HCOONH_4$ buffer in 75:25 isopropanol/water solution. Although such a post column addition dilutes the sample, it provides stable electrostatic conditions for the mass spectrometer, decreases the chance of *n*-hexane explosion, and introduces buffer ions for efficient APCI. Both scan and SIM modes were used to detect the product ions of the mass spectra. The characteristic $[M - OH]^+$ originating from fragmentation of the alcohols by dehydroxylation dominated the mass spectra of the products and were most frequently monitored in the SIM mode.

The absolute configuration of the reaction products was determined based on commercially available standards (either (*S*) or (*R*) isomers) or self-synthesized standards. In some cases where no commercial chiral standards were available and no pure products were accessible by our synthetic reductive procedures (see the Organic synthesis of standards section), the hypothetic configurations of the products were established based on a quantitative structure–enantioselective retention relationship (QSERR) model previously obtained,[10] combined with the retention times of fractions from racemic standards. Up-to-date, this approach proved to be effective in predicting the retention orders for a wide range of the ethylbenzene derivatives.

Flexible docking

The enzyme–substrate complex with 4-ethylphenol (**4**) was obtained in a flexible docking performed in Discovery Studio 3.5 (Accelrys) according to the procedure previously described.[23] A structure of EbDH α subunit with cofactor geometry obtained in QM/MM optimization was used as the receptor. The whole model was typed with a CHARMm force field (c36b2)[29] and MM point charges were calculated according to the Momany–Rone scheme.[30] The MM point charges for the substrate, the Mo cofactor, and the iron–sulfur cluster present in the α subunit of EbDH were fitted to the electrostatic potential according to the Merz–Singh–Kollman scheme.[31,32]

The initial position of the ligand was taken from an overlay with the position of ethylbenzene in the transition state associated with C–H activation (**TS1**).[23] Then, the geometry of 4-ethylphenol and all amino acid residues penetrating a 5 Å radius from the substrate were minimized. Thus, the obtained position of the substrate was used in DFT modelling.

Small cluster DFT modelling

The DFT cluster modelling was performed in Gaussian 09[33] according to the procedure previously established.[7,13] The choice of DFT follows from its suitability to adequately describe reaction pathways at a reasonable computational cost.[34,35] The Gaussian 09[33] package was used with a spin-unrestricted B3LYP functional.[36] Geometry optimization and vibration calculations were conducted with the 6-31G(d,p) basis set for light atoms and the LANL2DZ effective core potential and basis set for Mo. For a proper description of homolytic C–H cleavage, the α–β orbital symmetry was broken with a triplet solution in the intermediate product (**I**), followed by conversion to a singlet state. The transition states were localized by potential energy scans along the reaction coordinates followed by full optimization of transition state (TS) geometries using the Berny algorithm. Single point energies were calculated with the lacv3p** basis, both in gas phase and in a model solvent (assuming a polarized continuum model with $\varepsilon = 4$[37]) to correct for a continuous phase present in the enzyme active site. The obtained electronic energies were corrected by including zero point energies (ZPEs) obtained from B3LYP/6-31G(d,p) frequency calculations and employing a scaling factor of 0.98. The stable[38] check was performed for each single point energy calculation, and showed that there are no lower-energy states for the obtained geometries of stationary points. The energy differences

Table 1. LC–MS analyses of EbDH reaction mixtures of OH and NH_2 substituted substrates.

No.	Substrate	No.	Product	*S* (%)	*R* (%)	% ee	QSERR	IPA/*n*-hexane
1	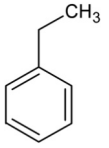 Ethylbenzene	**I**	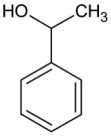 1-Phenylethanol	100	0	100		10:90
2	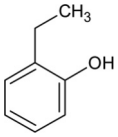 2-Ethylphenol	**II**	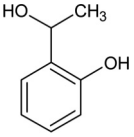 2-(1-Hydroxyethyl)phenol	100	0	100		15:85
3	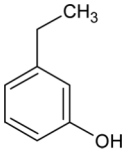 3-Ethylphenol	**III**	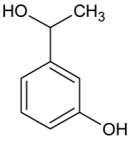 3-(1-Hydroxyethyl)phenol	100	0	100		15:85
4	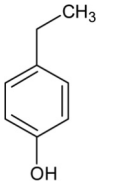 4-Ethylphenol	**IV**	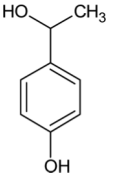 4-(1-Hydroxyethyl)phenol	87–90	13–10	74–80		15:85
5	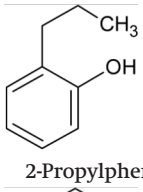 2-Propylphenol	**V**	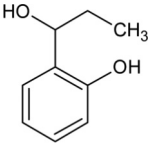 2-(1-Hydroxyprop-1-yl)phenol			100	*S*	10:90
6	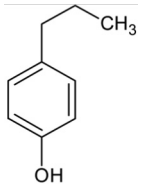 4-Propylphenol	**VI**	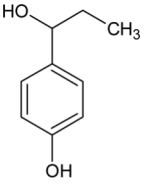 4-(1-Hydroxyprop-1-yl)phenol	95	5	90		15:85
7	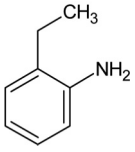 2-Ethylaniline	**VII**	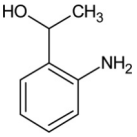 1-(2-Aminophenyl)ethanol			100		20:80
8	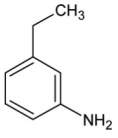 3-Ethylaniline	**VIII**	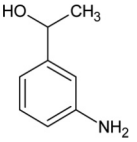 1-(3-Aminophenyl)ethanol			100	*S*	35:65
9	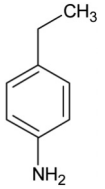 4-Ethylaniline	**IX**	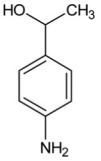 1-(4-Aminophenyl)ethanol			80–94	*S*	30:70

Table 1 (*concluded*).

No.	Substrate	No.	Product	*S* (%)	*R* (%)	% ee	QSERR	IPA/*n*-hexane
10	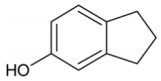 2,3-Dihydro-1*H*-inden-5-ol	**Xa**	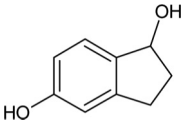 2,3-Dihydro-1*H*-indene-1,5-diol (66%)	55	45	10		15:85
		Xb	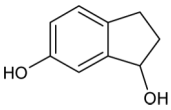 2,3-Dihydro-1*H*-indene-1,6-diol (33%)			100		15:85
11	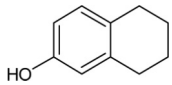 5,6,7,8-Tetrahydronaphthalen-2-ol	**XIa**	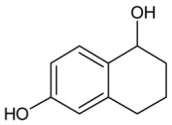 1,2,3,4-Tetrahydronaphthalene-1,6-diol (53%)			8	*S*	10:90
		XIb	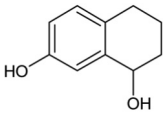 1,2,3,4-Tetrahydronaphthalene-1,7-diol (47%)			100		
12	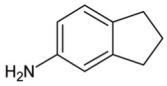 2,3-Dihydro-1*H*-inden-5-amine	**XIIa**	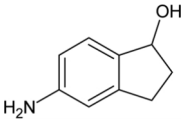 5-Amino-2,3-dihydro-1*H*-inden-1-ol			3–23	*S*	15:85
		XIIIb	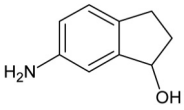 6-Amino-2,3-dihydro-1*H*-inden-1-ol*			100	*S*	15:85

Note: *S*/*R* (%) amount of isomers, identified based on chiral standards, percent enantiomeric excess (% ee), quantitative structure–enantioselective retention relationship (QSERR) identification of the major fraction based on the QSERR model,[10] and isopropanol (IPA)/*n*-hexane composition of mobile phase in LC chiral chromatography are presented.

were related to the enzyme substrate model (S) in which the position of 4-ethylphenol was derived from flexible docking. To ensure a similar position of the substrate in the cluster model as in the enzyme active site, the optimization was performed with an additional constraint between the Mo=O ligand and benzyl carbon atom. The transition state describing water displacement from Asp[485] by the quinone ethide intermediate was obtained with a smaller cluster model containing an Asp residue, water molecule, and substrate intermediate.

Thermochemical calculations

Simple thermochemical descriptors relating ΔG of carbocation formation from a particular substrate to ΔG of carbocation formation from ethylbenzene (i.e., $\Delta\Delta G$ values of the respective carbocations) were calculated in Gaussian 09 at the B3LYP/6-31G(d,p) level of theory for isolated organic compounds according to a previously established protocol.[39]

Cluster model

To address the modified reaction pathway for 4-ethylphenol (**4**), the usual "high pH" cluster model[7,13] was expanded by the side chain of Asp[485] (modelled as acetic acid) and a water molecule (Fig. 3). The potential formation of a *p*-quinone ethide intermediate (i.e., 4-ethylidenecyclohexa-2,5-dien-1-one) from 4-ethylphenol (**4**) and a respective *p*-ethide of cyclohexadienimine (4-ethylidenecyclohexa-2,5-dien-1-imine) from 4-ethylaniline (**5**) as reaction intermediates was studied with a cluster model, as was the cofactor-assisted reaction of the quinone ethide with a water molecule leading to the formation of both enantiomers of 4-(1-hydroxyethyl)phenol (**IV**).

Results

Chromatographic studies

The results of chiral LC–MS analysis of EbDH reaction mixtures are shown in Table 1. (*S*)-Alcohol products with 100% ee (within the detection limit) were observed for ethylbenzene (**1**), 2- and 3-ethylphenol (**2** and **3**, respectively), 2-propylphenol (**5**), and 2- and 3-ethylanilines (**7** and **8**, respectively). A decrease of enantioselectivity of EbDH-catalyzed hydroxylations was observed in the presence of OH and NH_2 substituents in the para position. This was experimentally confirmed with the phenolic compounds 4-ethylphenol (**4**, 74%–80% ee), 4-propylphenol (**6**, 95% ee), 2,3-dihydro-1*H*-inden-5-ol (**10**, 10% ee), and 5,6,7,8-tetrahydronaphthalen-2-ol (**11**, 8% ee) and the amines 4-ethylaniline

Fig. 3. The small cluster model of the active site of EbDH used for DFT calculations. (A) Schematic representation (gray atoms indicate frozen coordinates). (B) 3D structure of the active site with bound 4-ethylphenol (**4**) as a substrate (the dotted line represents an additional constraint used in optimization of the **S** state).

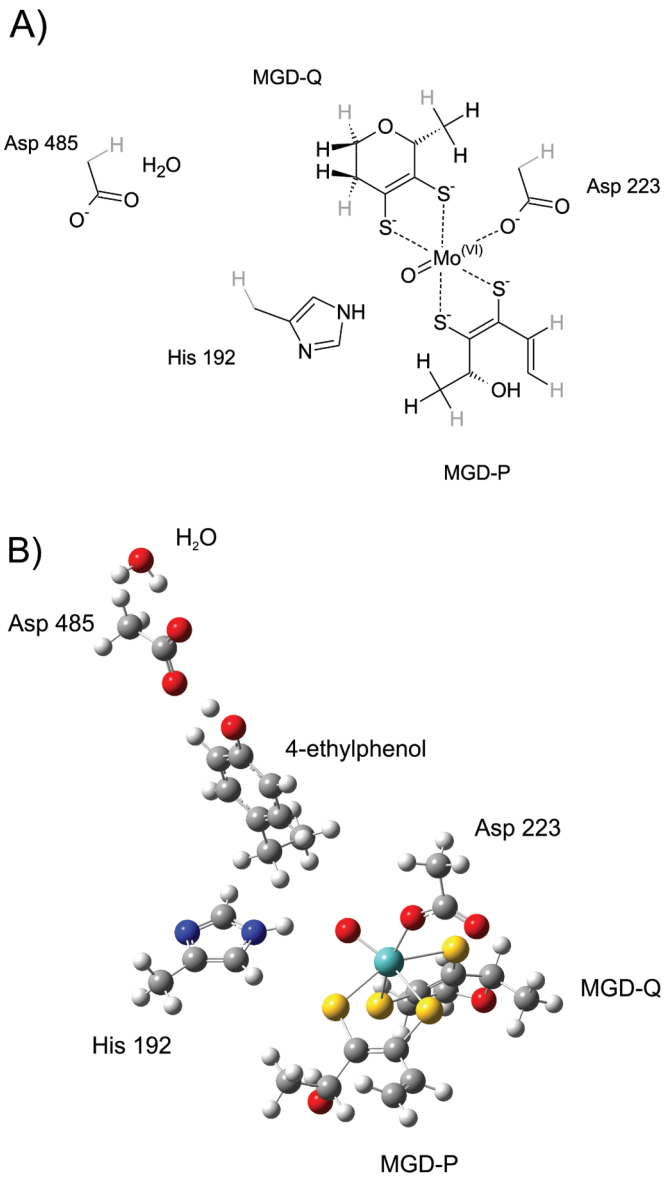

(**9**, 80%–94% ee) and 2,3-dihydro-1*H*-inden-5-amine (**12**, 3%–23% ee). For the substituted 2,3-dihydro-1*H*-indene and tetrahydronaphthalene derivatives (**10**, **11**, and **12**), only the major product peaks split into the two enantiomers during chiral LC, whereas additional minor product peaks showing the same MS spectra did not split up. These latter products were assigned as hydroxylation products of the alternative benzylic carbon of the alicyclic rings, which is in the meta position relative to the hydroxyl or amino substituents. The presence of only one enantiomer and coelution of the conversion product from **X** with the synthesized standard (*S*)-**Xb** confirmed the (*S*) chirality of this product and suggested that this is also the case for **XIb** and **XIIb**.

From the varying levels of enantioselectivity observed with 4-ethylphenol (**4**), 4-ethylaniline (**9**), and 2,3-dihydro-1*H*-inden-5-amine (**12**) in different experiments (Table 1), we assumed that variations in enzyme preparations or reaction conditions may influence the enantiomeric purity of the product. Based on the proposed hypothesis of an alternative reaction pathway involved under these conditions (see below), the % ee values might be sensitive to the pH conditions. Therefore, we determined the % ee values of the products from some of these compounds at pH values between 7 and 8. A systematic trend was observed for all three investigated compounds, which appeared to be hydroxylated with a higher stereoselectivity with increasing pH (Table 2).

Table 2. pH-dependence of hydroxylation enantioselectivity: enantiomeric excesses for the conversion of 4-ethylphenol (**4**), 4-ethylaniline (**9**), and 2,3-dihydro-1*H*-inden-5-amine (**12**).

	pH		
Substrate	7.0	7.5	8.0
4-Ethylphenol	74%	79%	80.2%
4-Ethylaniline	80%	92%	96%
2,3-Dihydro-1*H*-inden-5-amine	3%	8%	23%

Note: Values are the % enantiomeric excess of (*S*) isomers.

Modelling approaches to explain the loss of enantioselectivity for *p*-hydroxy- or *p*-amino-substituted substrates

The observed loss of reaction enantioselectivity may be explained with a modified reaction mechanism for *p*-OH- or *p*-NH_2-substituted compounds, which involves the formation of quinone ethide/imine intermediates and the nonenantioselective addition of H_2O. The proposed reaction was modelled by DFT as previously reported,[7,13] but using an extended model that included the side chain of Asp^{485} (see Fig. 3).

The reaction starts with the usual radical cleavage of the pro(*S*) C–H bond (**TS1**) leading to the radical intermediate (**I1**) as shown in our previous studies.[13] The geometry of **TS1** is similar to that previously reported (see Fig. S1 in the Supplementary data), with the exception of the H-bonding interactions of the *p*-OH group with Asp^{485} and a water molecule. The next step is associated with a transfer of the second electron, which leads to formation of a carbonation intermediate and reduction of the cofactor to the Mo(IV) state. At that point (**I1**), the reaction can either proceed through the conventional steps (OH rebound via transition state **TS2**, see Fig. 7A) to yield 4-((*S*)-1-hydroxyethyl)phenol and the reduced pentacoordinate molybdenum cofactor (MoCo; **P1**) (Fig. 4) or, in an alternative route, the carbocation may form a quinone ethide intermediate (**I2**). In the conventional pathway, the reaction cycle is closed by the release of the product and coordination of a water molecule to the active site, followed by oxidation of the cofactor with concomitant loss of two protons, which restores the catalytically active Mo(VI)=O species.

Quinone ethide formation should be greatly aided by interaction with the Asp^{485} residue, which may accept the phenolic proton. To obtain such a species (**I2**), a second electron has to be transferred from the radical substrate to the Mo atom and the phenolic proton must be shifted to the nucleophilic acceptor. Our modelling showed that both the carboxylic group of Asp^{485} and a water molecule hydrogen bonded to that group can act as proton acceptors. The actual transition from radical **I1** to quinone ethide **I2** (**TS3**) was characterized for the structure where the water molecule acts as an intermediary between the phenol OH group and Asp^{485} residue. Along the reaction coordinate (shift of a proton between oxygen atoms), spin density on the substrate gradually decreases, i.e., an electron is transferred in **TS3**. This proton-coupled electron transfer is also associated with a gradual decrease of the S_1–S_2–S_3–S_4 dihedral angle, which indicates a reduction of the molybdenum atom from Mo(V) to Mo(IV). In the transition state, two protons are being shifted, one from phenol to water and a second from water to Asp^{485}, yielding a protonated carboxylic group and quionon ethide. The actual energy barrier associated with the formation of the quinone ethide turns out to be very small (6 kJ/mol) and disappears when ZPE corrections are

Fig. 4. Schematic representation of a conventional reaction pathway for 4-ethylphenol (**4**). **S**, enzyme substrate complex; **TS1**, C–H activation transition state; **I1**, radical intermediate; **TS2**, OH rebound transition state; **P1**, *S* product with pentacoordiante MoCo; **I2**, quinone ethide intermediate.

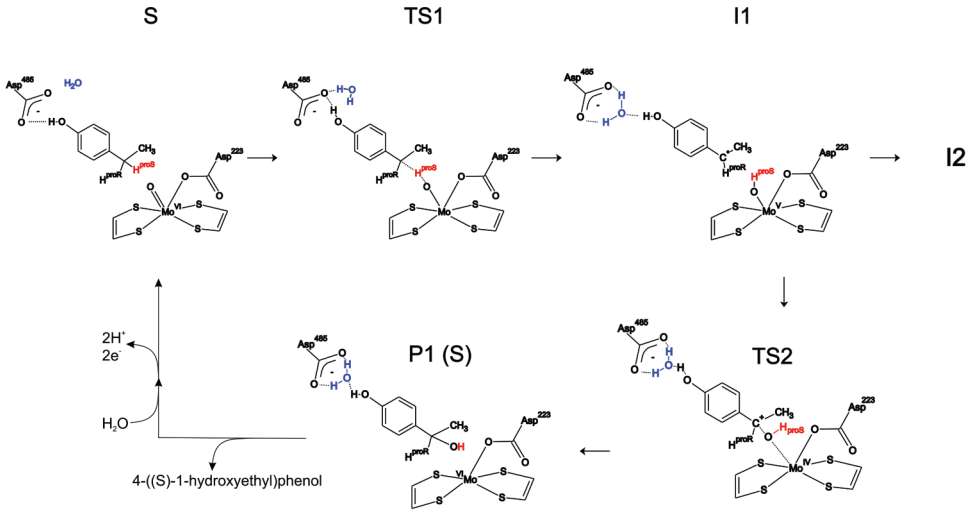

introduced (**TS3** energy is lower than **I1** by 2 kJ/mol). The quinone ethide state (**I2**) is significantly more stable than the **I1** radical intermediate ($\Delta(E + ZPE) = -31.4$ kJ/mol).

The quinone ethide can further react along four different pathways. It can either displace the water molecule from its hydrogen bond interaction with the Asp^{485} residue and mobilize it for addition to the C=C double bond, or a water molecule from the solvent may enter the active site and become available for the reaction (see the Supplementary data). The energy barrier for the water displacement, assessed from calculation on the smaller model, is in the range of 17 kJ/mol (**I2**–**I3**, energy of 4.4 kJ/mol). The freed water molecule can either form energetically favourable interactions with the Mo–OH ligand (**I3**) or energetically neutral interactions with the carboxylic oxygen atoms of Asp^{223} (**I4**) (see Fig. 5). The formation of **I3** is associated with lowering of the system energy by –15 kJ/mol, whereas formation of **I4** requires 1.8 kJ/mol more energy compared to **I2**. These intermediates contain a water molecule capable of forming strong H bonds with nucleophilic acceptors that can attack the C1 atom of the quinone ethide. The orientation of the quinone in **I3** allows an easy approach of H_2O from either side of the benzyl carbon atom, which results in pro(*S*) and pro(*R*) transition states (pro(*S*) and pro(*R*) **TS4**) leading to the formation of *S* and *R* products (**P2*S*** and **P3*R***), respectively (Fig. 6A and Figs. 7C, D). In either case, the water molecule donates one of its protons to the Mo–OH ligand concomitantly to hydrating the double bond, while Asp^{485} reprotonates the quinone group of the intermediate. It seems that the hydrogen bond between Mo–OH and the water molecule has a crucial role in activating the latter for the nucleophilic attack. The transition structures leading to both enantiomers exhibit C1–O distances of around 2.0 Å, whereas the ethyl side chain is either directed into the empty hydrophobic cavity (for the pro(*S*) conformation) or in the opposite direction.

Due to steric factors, the Asp^{223}-assisted attack of a water molecule is only possible from the pro(*R*) side, yielding transition state **TS5** in which the (*R*)-alcohol is formed with the ethyl side chain pointing toward the hydrophobic pocket (Fig. 6B). Similarly to **TS4**, the concomitant protonation of the quinone results in restoration of the phenolic aromatic ring. This pathway leads to species **P4** with a hexacoordinate molybdenum cofactor and protonated Asp^{223}.

Finally, a fourth pathway is possible that involves direct transition from **I2** to the product (**P1**). For this reaction route, we assume that the quinone intermediate does not displace a water molecule from Asp^{485} but instead approaches the Mo–OH ligand while forming a transition state (**TS6**) similar to that observed in **TS2** (Fig. 6C and Figs. 7A, B). Like in the conventional OH rebound model for ethylbenzene, the steric interactions in the active site would strongly favour a pro(*S*) orientation over pro(*R*). The transition state, one proton is shuttled back from Asp^{485} to a water molecule and another one from a water molecule to the quinone, while the OH^- group is directly transferred from Mo to the C1 carbon atom. This reaction yields the product in *S* configuration and pentacoordinated MoCo identical to that proposed for the conventional pathway (**P1*S***).

An analysis of energy profiles (Table 3, Fig. 8) of the resulting modified mechanisms indicates that C–H activation is the rate limiting step of the whole process (**TS1**, 107.6 kJ/mol). Moreover, the energy of a "standard" rebound reaction of the intermediate (in a pro(*S*) orientation) with the OH ligand of the Mo cofactor (**TS2**, 35 kJ/mol) is significantly higher than the energy of the alternative pathway involving water addition of a quinone ethide intermediate either in the pro(*S*) or pro(*R*) conformation (**TS4** energies are 13 and 14 kJ/mol for the pro(*S*) and pro(*R*) pathway, respectively) or the energy for the reaction of the quinone ethide with the Mo–OH ligand in the pro(*S*) orientation (**TS6**, 20.9 kJ/mol). As there is no energy barrier between **I1** and **I2**, the radical intermediate will very likely evolve into the quinone ethide form instead of directly reacting with the Mo–OH ligand (OH rebound). From this (quinone ethide-bound) stage, various scenarios are energetically accessible. The water molecule may either be displaced from its position at the Asp^{485}, further stabilizing the system by –15 kJ/mol, or yet another water molecule may bind by H-bond bridges to the Mocofactor. In the former scenario, the absolute barriers associated with **TS4**s are calculated as 40.5 and 41.4 kJ/mol (for pro(*S*) and pro(*R*), respectively), which are approximately 8 kJ/mol higher than those for the reaction of the quinone ethide with the hydroxyl ligand of the molybdenum (**TS6**). However, these energy differences are mainly due to system stabilization after water displacement. If another water molecule is involved in the reaction, both types of transition states attain a similar energy. In such a scenario, the barrier associated with **TS6** is only 2 and 6.2 kJ/mol lower than that with **TS4** for pro(*S*) and pro(*R*) transition states, respectively (see the Supplementary data).

On the other hand, the reaction with a water molecule interacting with Asp^{223} is calculated to be associated with a significantly higher energy barrier (**TS5**, 50.7 kJ/mol; absolute barrier of 63.2 kJ/mol).

Finally, it should be underlined that reaction pathways associated with water attack on the quinone ethide (**TS4**) yield hexa-

Fig. 5. Schematic representation of the steps leading to a proposed alternative pathway: formation of the quinone intermediate and three different reaction intermediates. **TS3**, transition state associated with the electron transfer and formation of quinone ethide; **I1**, radical intermediate; **I2**, quinone ethide intermediate with water bound to Asp^{485}; **I3**, quinone ethide intermediate with water bound to Mo–OH; **I4**, quinone ethide intermediate with water bound to Asp^{223}.

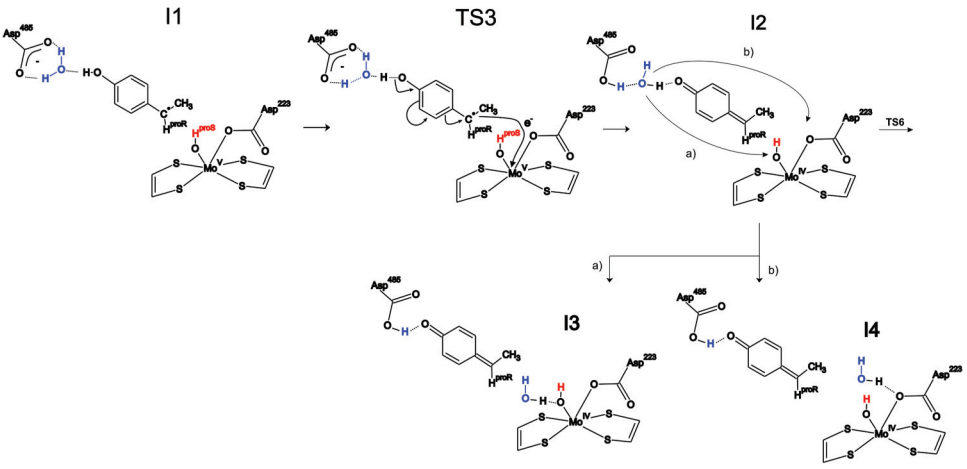

Fig. 6. Four alternative reaction pathways of the proposed quinone intermediate: (A) Reactions involving a water molecule interacting with Mo–OH: **TS4**, it shows either a (*a*) pro(*S*) or (*b*) pro(*R*) transition state after the benzylic carbon atom is attacked by water; **P2**, the *S* product with a hexacoordinated Mo–H_2O; **P3**, the *R* product with a hexacoordinated Mo–H_2O. (B) The reaction involving a water molecule interacting with Mo–Asp^{223}: **TS5**, the pro(*R*) transition state after water attack on the benzylic carbon atom; **P4**, the *R* product with a hexacoordinated Mo–OH and protonated Asp^{223}. (C) The direct reaction of the quinone ethide intermediate with the Mo–OH ligand: **TS6**, transition state; **P1**, the *S* product and pentacoordinated MoCo.

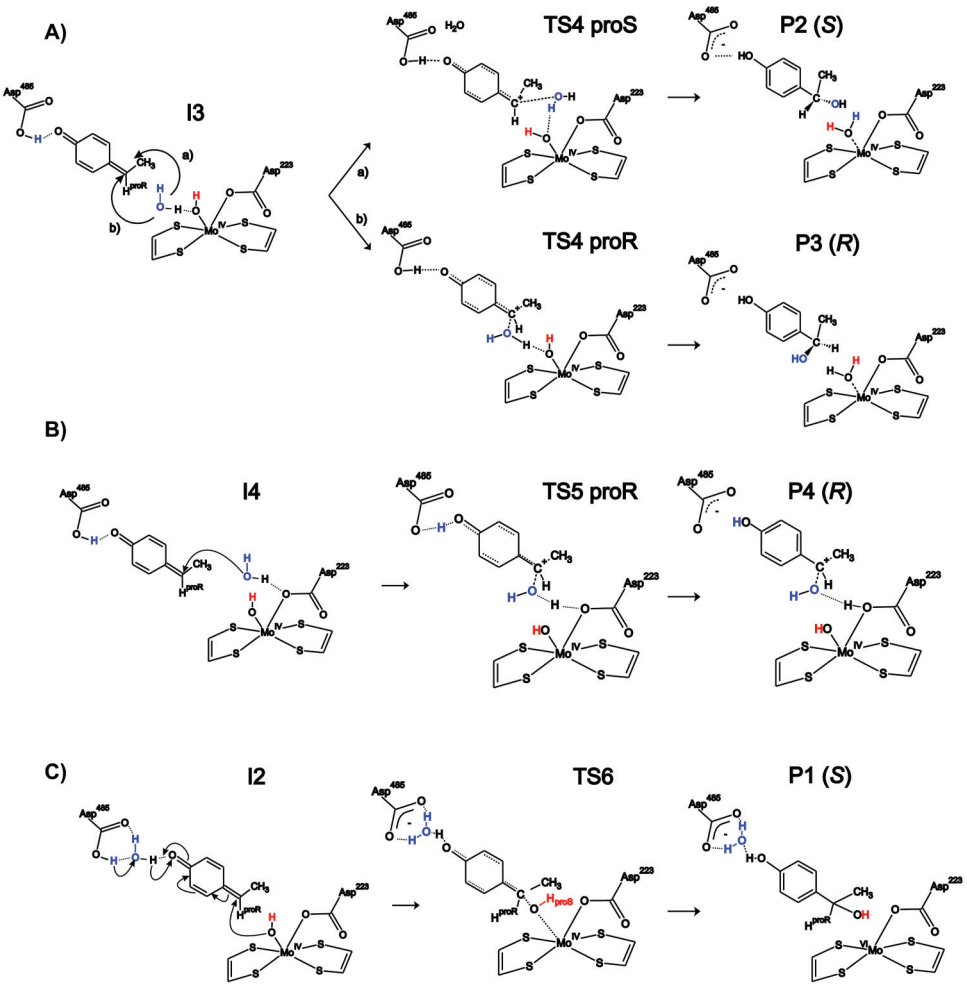

Table 3. Energy differences calculated for the 4-ethylphenol (**4**) reaction via the conventional and modified proposed pathways.

Stationary point	Δ(*E* + ZPE) gas phase (kJ/mol)	Δ(*E* + ZPE) solvent (kJ/mol)
S	*0*	*0*
TS1	*107.0*	*107.6*
I1	*7.5*	*18.9*
TS2	*29.7*	*34.9*
P1	*–35.6*	*–33.0*
TS3	14.7	17.0
I2	–2.8	–12.5
I2–I3[a]	18.0	4.4
I3	–12.8	–27.5
TS4 pro(*S*)	20.9	13.0
TS4 pro(*R*)	22.7	14.2
P2*S*	–55.7	–55.9
P3*R*	–54.4	–53.4
I4	–0.9	–10.8
TS5 pro(*R*)	60.4	50.7
P4*R*	26.9	18.0
TS6	19.5	20.9

Note: The conventional pathway is marked in italic.
[a]Energy estimated from a smaller model.

coordinated MoCo with a water ligand, which is ready for deprotonation and restoration of the catalytically active Mo(VI)=O species. As a result, **P2** and **P3** have significantly lower energies than **P1** (by 23 kJ/mol).

In the case of 4-ethylaniline (**9**), a similar spontaneous formation of 4-ethylidenecyclohexa-2,5-dien-1-imine (Δ(*E* + ZPE) = –9.5 kJ/mol) may occur after the transfer of the second electron from the radical intermediate, providing an analogous explanation for the low enantioselectivity (see Fig. S3 in the Supplementary data for the structure of the imine intermediate). However, we did not calculate the complete pathway for this substrate.

Discussion

The preliminary modelling studies (data not shown) conducted for the conventional reaction pathway of EbDH (ethylbenzene hydroxylation) indicated that the high enantioselectivity of the reaction is imposed by stereoselective activation of a C–H bond followed by a rapid reaction of a carbocation intermediate with the hydroxyl group of Mo–Co. The second step of the hydroxylation mechanism (i.e., OH rebound) is believed to be less enantioselective, because the C1···OH–Mo bond length in **TS2** is longer than the H···O–Mo distance involved in the C–H activation process (**TS1**). Due to the longer distance between the reactant and MoCo, both pro(*R*) and pro(*S*) conformations of **TS2** may occur in the active site as the ethyl side change is further remote from the residues determining enantioselective steric interactions.[14] However, for most substrates the **I1** intermediates seem to be short-lived species, and their potential pro(*S*)-pro(*R*)-rotation does not seem to contribute significantly to increasing the production of (*R*)-alcohols through the pro(*R*) **TS2** OH rebound process.

Therefore, the observed severe loss of reaction enantioselectivity in the case of para-substituted phenols and anilines is most probably associated with changes in the reaction pathway of the second part of the reaction, i.e., after the enantioselective C–H activation.

The enantioselectivity of EbDH with substrates substituted with NH_2 or OH groups is clearly dependent on directional interactions of those substituents with a reaction site at the benzylic carbon atom. In contrast to the para-substituted compounds, meta- and ortho-substituted analogs are exclusively converted to (*S*)-alcohols. This property becomes especially prominent in the case of substrates with two possible hydroxylation sites either in the *m*- or *p*-position to a hydroxyl or amino substituent (**10**, **11**, **12**). The carbon in the meta position is always hydroxylated to a pure (*S*)-alcohol, whereas the carbon in the para position is hydroxylated to mixtures of (*S*)- and (*R*)-alcohols. Besides the positioning of the substituent to be hydroxylated, the ability to subtract a proton from the OH/NH_2 substituent seems of utmost importance. Indeed, hydroxylation of the nondissociable analog 1-ethyl-4-methoxybenzene proceeds with 100% ee to the (*S*)-alcohol.[10]

It was our intention to demonstrate by modelling studies that the alternative reaction pathway(s) involving deprotonation of the phenolic/anilinic group is feasible and may lead through energetically accessible barriers to an increased amount of (*R*)-alcohols. Our hypothetic reaction mechanism involves stabilization of the reactive radical intermediate (**I1**) into a form of the quinone ethide intermediate (**I2**). Such an intermediate may be formed by a direct proton abstraction from the para substituent of the radical or the short-lived carbocation intermediate by the Asp^{485} residue or via a water molecule interacting through H bonds with the carboxylic group of Asp^{485}. Both processes are energetically favourable, but the latter seems more probable due to the presence of a water molecule in the vicinity of Asp^{485} and its likely interaction with the phenolic group during C–H activation (**TS1**). The calculations showed no energy barrier between the radical (**I1**) and quinone intermediates (**I2**), suggesting a spontaneous proton-coupled electron transfer from the radical intermediate to the Mo–Co together with deprotonation of the phenolic group. The formation of a stabilized quinone ethide intermediate may then be followed by a nonenantioselective water addition reaction proceeding with almost the same energy barriers for pro(*S*) and pro(*R*) orientations (13 vs 14.2 kJ/mol), or by a slightly enantioselective direct addition of the hydroxyl group of Mo–OH (most probably preferentially yielding the (*S*)-alcohol). The absolute barriers of both pathways (especially assuming the involvement of a second water molecule) are in the same range with a slight preference for the enantioselective attack of Mo–OH at the quinone ethide. This result is in agreement with experiments which still show some excess of the (*S*)-enantiomer over the (*R*).

The modelling also showed that the carboxylic group of Asp^{223}, which coordinates Mo as a protein-derived ligand, can potentially bind another water molecule (**I4**), which in turn may attack the quinone ethide intermediate. However, this process is associated with a much higher energy barrier (**TS5**, 50.7 kJ/mol), and the product (**P3**) exhibits a higher energy than those involved in the above discussed pathways. Thus, we conclude that the latter mechanism does not significantly contribute to the observed effect.

One can also imagine that a water molecule may approach the quinone ethide from the pro(*R*) side of the molecule without interacting with either Mo–OH or Asp^{223}. In such a situation, the water would not be activated for nucleophilic attack and the resulting product would be a protonated alcohol. However, this scenario would be energetically unfavorable and therefore was not considered in this paper.

The hypothetical alternative quinone–water reaction pathway presented above is also supported by the observed pH dependence on enantioselectivity for **4**, **9**, and **12**, which may reflect the (de)protonation grade of Asp^{485} and its ability to abstract the phenolic proton, or its ability to reprotonate the quinone ethide (imine) during H_2O attack on the C=C bond.

Another hypothetical explanation for the observed loss of enantioselectivity could imply an extended lifespan of the carbocation intermediate due to stabilizing effects of the *p*-OH or *p*-NH_2 substituents. This hypothesis would reject the formation of quinone/imine ethide intermediates (**I2**). The extended stabilization of a carbocation intermediate might facilitate rotation of the activated form in the active site and formation of the (*R*)-alcohol via the standard OH rebound process. The Hammett σ^{+}_{para}parameters for *p*-OH and *p*-NH_2 (–0.92 and –1.3, respectively), as well as calculated $\Delta\Delta G_{carbocation}$ values for phenols and anilines (–46.6, –48.8,

Fig. 7. Geometries of the transition states of alcohol formation from 4-ethylphenol: (A) the conventional pro(*S*)-oriented OH rebound reaction (**TS2**); (B) the OH rebound reaction to the quinone ethide intermidiate (**TS6**); (C) and (D) the modified pro(*S*)- and pro(*R*)-oriented **TS4** structures of the reaction pathways with the involved water molecules, respectively. Structures of all stationary points are available in the Supplementary data (Figs. S3 and S4).

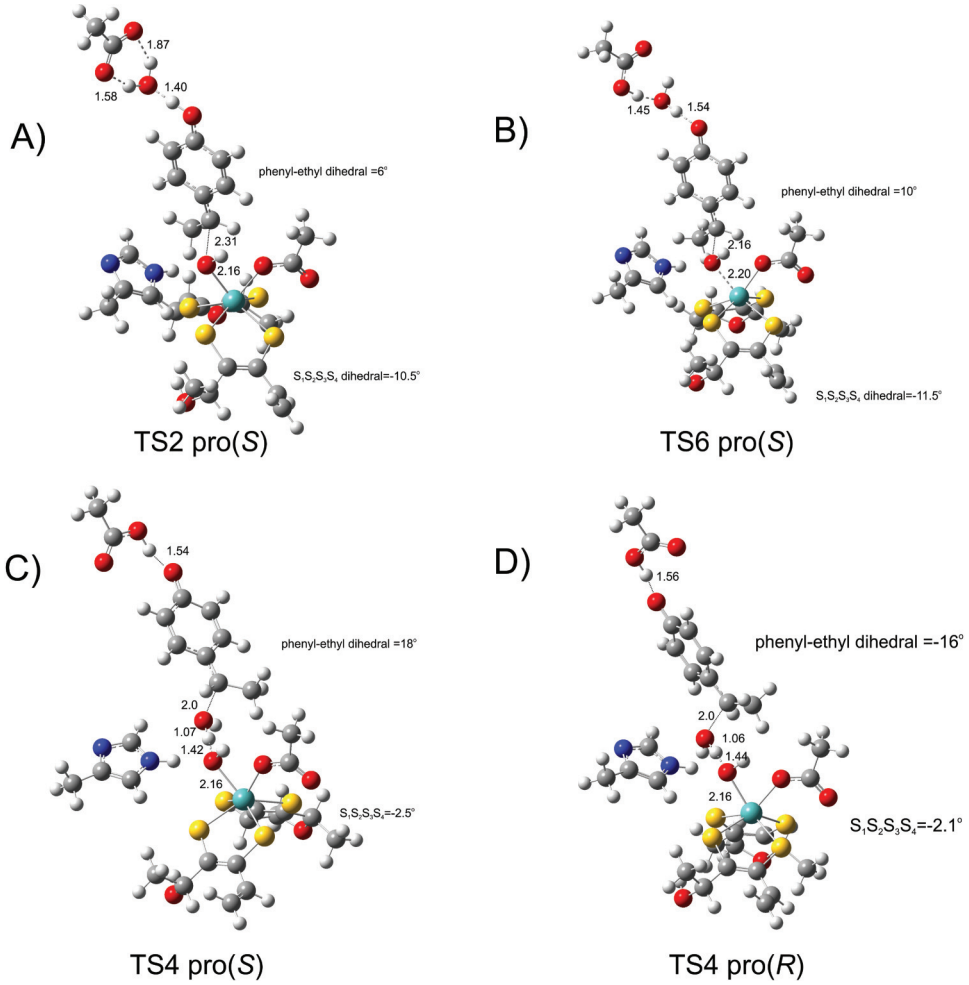

Fig. 8. Energy diagram of reaction pathways (Δ(*E* + ZPE) solvent): Black, conventional pathway (only *S* enantiomer); green, quinone ethide pathway with H_2O bound to Mo–OH (dark green - pro(*S*) and light green - pro(*R*) pathways); blue, quinone ethide pathway with H_2O bound at Asp^{223}; red, quinone ethide pathway with hydroxyl transfer from Mo–OH (only *S* enantiomer). The energy scale is in kJ/mol.

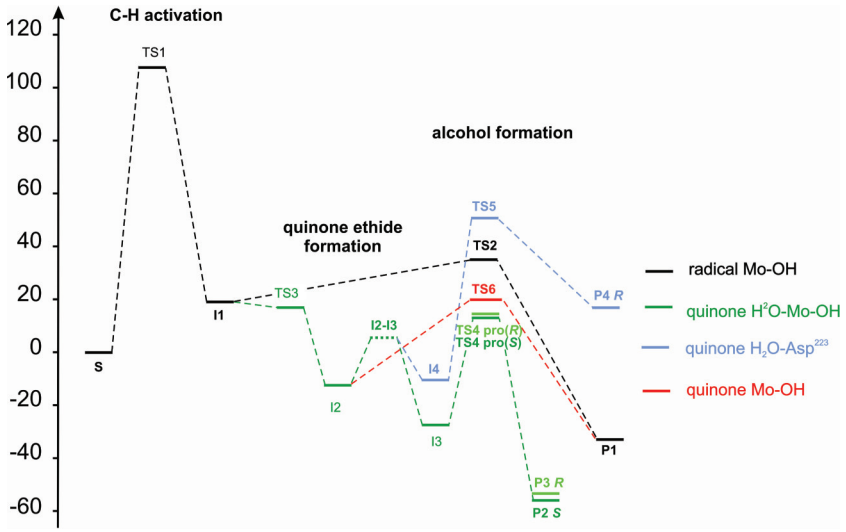

–70, –74, –97, and –118 kJ/mol for **4**, **6**, **10**, **11**, **9**, and **12**, respectively) indicate that *p*-OH or *p*-NH_2 groups should indeed principally stabilize carbocation species. However, this hypothesis is in contrast with the observation that 1-ethyl-4-methoxybenzene, which should also produce a strongly resonance-stabilized carbonation intermediate (σ^{+}_{para} = –0.78, $\Delta\Delta G_{carbocation}$ = –60 kJ/mol), is hydroxylated completely enantioselectivly (100% (*S*)).[10] Moreover, the significant loss of enantioselectivity due to rotation of the activated 4-ethylphenol would require much higher energy barriers between **I1** and **TS2** than those calculated for ethylbenzene. Our calculations indicate, however, that these barriers are approximately the same for both substrates (~40 kJ/mol). Therefore, the mere stabilization of a carbocation intermediate and its increased probability to rotate in the active site does not seem to be a primary reason for enantioselectivity loss, especially in the case of OH and NH_2 para-substituted compounds.

Summing up, we suggest that the loss of reaction enantioselectivity for some EbDH substrates (e.g., 4-ethylphenol, 4-ethylaniline, or 2,3-dihydro-1*H*-inden-5-ol and 2,3-dihydro-1*H*-inden-5-amine) is caused by deprotonation of a carbocation intermediate at a hydroxyl or amino ligand in the para position yielding a quinone ethide intermidiate, followed by water addition to that intermediate.

Conclusions

The reaction mechanism of EbDH is extended by an alternative variant that comes into play for para-substituted alkylphenols and alkylanilines. The observed loss in enantioselectivity for these substrates may be best explained as a nonenantioselective side reaction of a stabilized quinone ethide intermediate with a water molecule activated by hydrogen bonding to Mo–OH. The involvement of proton transfer in the reaction was suggested by the observation of pH-dependent variations of the enantiomer compositions. This effect supported our hypothesis and may even be used to further optimize reaction conditions to modify stereoselectivity.

Supplementary data

Supplementary data (details of the product identification (Table S1), absolute energies of stationary points for the 4-ethylphenol pathway (Table S2), energy differences for the pathway with two water molecules (Table S3), figures of the stationary points for the 4-ethylphenol reaction pathway (Fig. S1), figures of the stationary points for the alternative pathway "quinone – Mo–OH–H_2O" (Fig. S2), figures of the stationary points for the alternative pathway "quinone – Mo–Asp^{223}–H_2O" (Fig. S3), figure of **TS6** for the alternative pathway "quinone – Mo–OH" (Fig. S4), figures of the stationary points for the alternative pathway quinone – $2H_2O$–OH–Mo Asp^{485} (Fig. S5), figure of the **I2** intermediate calculated for the 4-ethylaniline alternative pathway (Fig. S6), and figures of small cluster models used for evaluation of the **I2–I3** water displacement process (Fig. S7)) are available with the article through the journal Web site at http://nrcresearchpress.com/doi/suppl/10.1139/cjc-2012-0504.

Acknowledgements

The authors acknowledge the financial support of the priority program 1319 of the German Research Foundation (DFG), the excellence program The LOEWE Center for Synthetic Microbiology (LOEWE/SYNMIKRO) from the state of Hessen, Germany, the computational grant MNiSW/SGI3700/PAN/121/2006, the Marian Smoluchowski Krakow Research Consortium - a Leading National Research Centre KNOW supported by the Ministry of Science and Higher Education, the Polish National Science Center under grant N N204 269038, as well as the financial support of the project "Biotransformations for pharmaceutical and cosmetics industry" No. POIG.01.03.01-00-158/09-00, which is in part financed by the European Union (EU) within the European Regional Development Fund. Anna Wójcik acknowledges project "Kraków Interdisciplinary PhD – Project in Nanoscience and Advanced Nanostructures" operated within the Foundation for Polish Science MPD Programme and cofinanced by the EU European Regional Development Fund.

References

(1) Kniemeyer, O.; Heider, J. *J. Biol. Chem.* **2001**, *276* (24), 21381–21386. doi:10.1074/jbc.M101679200.
(2) Hille, R. The Mononuclear Molybdenum Enzymes. *Chem. Rev.* **1996**, *96* (7), 2757–2816. doi:10.1021/cr950061t.
(3) Johnson, H. A.; Pelletier, D. A.; Spormann, A. M. *J. Bacteriol.* **2001**, *183* (15), 4536–4542. doi:10.1128/JB.183.15.4536-4542.2001.
(4) Heider, J. *Curr. Opin. Chem. Biol.* **2007**, *11* (2), 188–194. doi:10.1016/j.cbpa.2007.02.027.
(5) Rabus, R.; Kube, M.; Heider, J.; Beck, A.; Heitmann, K.; Widdel, F.; Reinhardt, R. *Arch. Microbiol.* **2005**, *183* (1), 27–36. doi:10.1007/s00203-004-0742-9.
(6) Kloer, D. P.; Hagel, C.; Heider, J.; Schulz, G. E. *Structure* **2006**, *14* (9), 1377–1388. doi:10.1016/j.str.2006.07.001.
(7) Szaleniec, M.; Borowski, T.; Schuhle, K.; Witko, M.; Heider, J. *J. Am. Chem. Soc.* **2010**, *132* (17), 6014–6024. doi:10.1021/ja907208k.
(8) Szaleniec, M.; Witko, M.; Tadeusiewicz, R.; Goclon, J. *J. Comput. Aided Mol. Des.* **2006**, *20* (3), 145–157. doi:10.1007/s10822-006-9042-6.
(9) Szaleniec, M.; Hagel, C.; Menke, M.; Nowak, P.; Witko, M.; Heider, J. *Biochemistry* **2007**, *46* (25), 7637–7646. doi:10.1021/bi700633c.
(10) Szaleniec, M.; Dudzik, A.; Pawul, M.; Kozik, B. *J. Chromatogr. A* **2009**, *1216* (34), 6224–6235. doi:10.1016/j.chroma.2009.07.002.
(11) Knack, D.; Hagel, C.; Szaleniec, M.; Dudzik, A.; Salwinski, A.; Heider, J. *Appl. Environ. Microb.* **2012**, *78* (18), 6475–6482. doi:10.1128/aem.01551-12.
(12) Szaleniec, M. *Pharmacol. Rep.* **2012**, *64*, 511–531.
(13) Szaleniec, M.; Salwinski, A.; Borowski, T.; Heider, J.; Witko, M. *Int. J. Quantum Chem.* **2012**, *112* (8), 1990–1999. doi:10.1002/Qua.23143.
(14) Szaleniec, M.; Dudzik, A.; Tataruch, M.; Witko, M.; Knack, D.; Heider, J. *Enantioselective hydroxylation by ethylbenzene dehydrogenase – origins of enantioselectivity*; In *6th International Congress on Biocatalysis BIOCAT 2012, Hamburg*; 2012, p. 262
(15) Reider, P. J. *Advances in AIDS CHIMIA* **1997**, *51* (6), 306–308.
(16) Gen-Sheng, Y.; Jiang-Yan, X.; Zhi-Min, O.; Shan-Jing, Y. *Biotechnol. Lett.* **2009**, *31* (12), 1879–1883. doi:10.1007/s10529-009-0084-4.
(17) Suan, C.; Sarmidi, M. R. *J. Mol. Catal. B Enzym.* **2004**, *28* (2-3), 111–119. doi:10.1016/j.molcatb.2004.02.004.
(18) Hanson, R. L.; Goldberg, S.; Goswami, A.; Tully, T. P.; Patel, R. N. *Adv. Synth. Catal.* **2005**, *347* (7-8), 1073–1080. doi:10.1002/adsc.200505045.
(19) Kaneoya, M.; Uchida, M.; Yoshida, N.; Miyazawa, K. *1-Phenyl-1-propanol derivatives*; *Edited by* EP; Chisso Corporation, CH DE FR GB IT LI SE; 1991, pp. 1–17.
(20) Pal, S.; Park, D.-H.; Plapp, B. V. *Chem-Biol. Interact.* **2009**, *178* (1–3), 16–23. doi:10.1016/j.cbi.2008.10.037.
(21) Uwai, K.; Konno, N.; Yasuta, Y.; Takeshita, M. *Bioorg. Med. Chem.* **2008**, *16* (3), 1084–1089. doi:10.1016/j.bmc.2007.10.096.
(22) Hopper, D. J.; Cottrell, L. *Appl. Environ. Microb.* **2003**, *69* (6), 3650–3652. doi:10.1128/Aem.69.6.3650-3652.2003.
(23) Knack, D. H.; Marshall, J. L.; Harlow, G. P.; Dudzik, A.; Szaleniec, M.; Liu, S. Y.; Heider, J. *Angew. Chem. Int. Ed. Eng.* **2013**, *52* (9), 2599–2601. doi:10.1002/anie.201208351.
(24) Kniemeyer, O.; Heider, J. *J. Biol. Chem.* **2001**, *276* (24), 21381–21386. doi:10.1074/jbc.M101679200.
(25) Kniemeyer, O.; Heider, J. *Arch. Microbiol.* **2001**, *176* (1-2), 129–135. doi:10.1007/s002030100303.
(26) Hoffken, H. W.; Duong, M.; Friedrich, T.; Breuer, M.; Hauer, B.; Reinhardt, R.; Rabus, R.; Heider, J. *Biochemistry* **2006**, *45* (1), 82–93. doi:10.1024/bi051596b.
(27) Alebic-Kolbah, T.; Paul Zavitsanos, A. *J. Chromatogr. A* **1997**, *759* (1-2), 65–77. doi:10.1016/s0021-9673(96)00756-x.
(28) Zavitsanos, A. P.; Alebic-Kolbah, T. *J. Chromatogr. A* **1998**, *794* (1-2), 45–56. doi:10.1016/s0021-9673(97)00892-3.
(29) Brooks, B. R.; Bruccoleri, R. E.; Olafson, B. D.; States, D. J.; Swaminathan, S.; Karplus, M. *J. Comput. Chem.* **1983**, *4* (2), 187–217. doi:10.1002/jcc.540040211.
(30) Momany, F. A.; Rone, R. *J. Comput. Chem.* **1992**, *13* (7), 888–900. doi:10.1002/jcc.540130714.
(31) Singh, U. C.; Kollman, P. A. *J. Comput. Chem.* **1984**, *5* (2), 129–145. doi:10.1002/jcc.540050204.
(32) Besler, B. H.; Merz, K. M.; Kollman, P. A. *J. Comput. Chem.* **1990**, *11* (4), 431–439.
(33) Frisch, M. J.; Trucks, G. W.; Schlegel, H. B.; Scuseria, G. E.; Robb, M. A.; Cheeseman, J. R.; Scalmani, G.; Barone, V.; Mennucci, B.; Petersson, G. A.; Nakatsuji, H.; Caricato, M.; Li, X.; Hratchian, H. P.; Izmaylov, A. F.; Bloino, J.; Zheng, G.; Sonnenberg, J. L.; Hada, M.; Ehara, M.; Toyota, K.; Fukuda, R.; Hasegawa, J.; Ishida, M.; Nakajima, T.; Honda, Y.; Kitao, O.; Nakai, H.; Vreven, T.; Montgomery, J. A., Jr.; Peralta, J. E.; Ogliaro, F.; Bearpark, M.; Heyd, J. J.; Brothers, E.; Kudin, K. N.; Staroverov, V. N.; Kobayashi, R.; Normand, J.; Raghavachari, K.; Rendell, A.; Burant, J. C.; Iyengar, S. S.; Tomasi, J.;Cossi, M.; Rega, N.; Millam, N. J.; Klene, M.; Knox, J. E.; Cross, J. B.; Bakken, V.; Adamo, C.; Jaramillo, J.; Gomperts, R.; Stratmann, R. E.; Yazyev, O.; Austin, A. J.; Cammi, R.; Pomelli, C.; Ochterski, J. W.; Martin, R. L.; Moro-

kuma, K.; Zakrzewski, V. G.; Voth, G. A.; Salvador, P.; Dannenberg, J. J.; Dapprich, S.; Daniels, A. D.; Farkas, Ö.; Foresman, J. B.; Ortiz, J. V.; Cioslowski, J.; Fox, D. J. *Gaussian 09 Revision A.01*; Gaussian, Inc., Wallingford CT, 2009.
(34) Rutkowska-Zbik, D.; Witko, M.; Serwicka, E. M. *Catalysis Today* **2011**, *169* (1), 10–15. doi:10.1016/j.cattod.2010.09.014.
(35) Rutkowska-Zbik, D.; Witko, M.; Serwicka, E. M. *Catalysis Today* **2004**, *91-2*, 137–141. doi:10.1016/j.cattod.2004.03.022.
(36) Becke, A. D. *J. Chem. Phys.* **1993**, *98* (7), 5648–5652. doi:10.1063/1.464913.
(37) Cossi, M.; Scalmani, G.; Rega, N.; Barone, V. *J. Chem. Phys.* **2002**, *117* (1), 43. doi:10.1063/1.1480445.
(38) Bauernschmitt, R.; Ahlrichs, R. *J. Chem. Phys.* **1996**, *104* (22), 9047–9052. doi:10.1063/1.471637.
(39) Szaleniec, M.; Witko, M.; Heider, J. *J. Mol. Catal. A Chem.* **2008**, *286* (1-2), 128–136. doi:10.1016/j.molcata.2008.02.016.